Letter

Quantum Hall effect and zero-resistance plateau in bulk HgTe

M. L. Savchenko,[1,2,*] D. A. Kozlov,[3,4] S. S. Krishtopenko,[5] N. N. Mikhailov,[4] S. A. Dvoretsky,[4] Z. D. Kvon,[4,6] A. Pimenov,[1] and D. Weiss[3]

[1]*Institute of Solid State Physics, Vienna University of Technology, 1040 Vienna, Austria*
[2]*Microsystems Division, Silicon Austria Labs, 9524 Villach, Austria*
[3]*Experimental and Applied Physics, University of Regensburg, D-93040 Regensburg, Germany*
[4]*Institute of Semiconductor Physics, Novosibirsk 630090, Russia*
[5]*Laboratoire Charles Coulomb (L2C), UMR 5221 CNRS-Université de Montpelier, Montpellier, France*
[6]*Physics Department, Novosibirsk State University, Novosibirsk 630090, Russia*

(Received 16 July 2025; accepted 20 October 2025; published 1 December 2025)

We investigate the quantum Hall effect (QHE) in a gated 1000-nm-thick HgTe film that nominally constitutes a three-dimensional system. Around the charge neutrality point (CNP), we observe a weak zero plateau in the Hall resistance, accompanied by a relatively small value of R_{xx} on the order of h/e^2. We demonstrate that the zero plateau arises from counterpropagating chiral electron-hole edge channels with suppressed interchannel scattering. This behavior resembles that of the quantum spin Hall effect; however, in our case, quasiballistic transport persists over macroscopic distances. We show that the QHE emerges within a two-dimensional (2D) accumulation layer near the gate, while the bulk of the film serves as an electron reservoir. Carrier exchange between the reservoir and the 2D layer gives rise to anomalous scaling of the QHE—not with respect to the CNP, but relative to the first electron plateau.

DOI: 10.1103/fc7w-cq8f

The quantum Hall effect (QHE) [1] stands as one of the most groundbreaking discoveries in physics in the latter half of the 20th century. It introduced the concept of the conductance quantum (e^2/h), offering a clear, simple, and highly precise demonstration of quantum mechanics at work. The profound significance and broad applicability of QHE have ensured that it remains a key area of both theoretical and experimental research. Current investigations primarily focus on realizing the QHE in emerging materials such as graphene [2], semimetals [3,4], and three-dimensional (3D) topological insulators (TIs) [5–7]. In graphene and semimetals, the behavior of the zero Landau level (LL), which manifests as zero Hall conductivity, $\sigma_{xy} = 0$, is of particular interest. Although several theoretical models address this phenomenon [8–11], no consensus has been reached regarding the realization of the zero plateau. In 3D TIs, topologically nontrivial and nondegenerate surface states exist independently of the position of the Fermi level [12,13]. If the bulk of such materials is insulating, the conducting surfaces are natural two-dimensional (2D) systems, exhibiting QHE originating from the surface states [5,6,14]. Another intriguing issue is the possibility of observing the half-integer QHE [15], which remains a topic of ongoing discussion. Furthermore, it has been suggested [16] that the QHE can be realized in 3D topological semimetals. Recently, the 3D QHE was demonstrated in bulk $ZrTe_5$ [17], a system that actually has a layered structure. Since this provides a completely different perspective on the formation of the QHE, further experiments in the field are eagerly anticipated, especially if they can be realized using existing systems.

Here we present an experimental study of a high-quality, gated 1000-nm-thick HgTe film. The film was grown by molecular beam epitaxy on a GaAs(013) substrate under the same conditions and with the same layer sequence as for typical 80 and 200 nm films [18,19]. A schematic cross-sectional view of the devices is shown in Fig. 1(a). The HgTe film thickness is approximately ten times larger than the pseudomorphic growth limit for HgTe on a CdTe substrate, which has a lattice constant 0.3% larger than that of HgTe [14,19]. Therefore, we conclude that the film under study is fully relaxed to its original lattice constant, rendering it a zero-gap semiconductor [20] with an inverted band structure hosting 3D carriers and topological surface electrons.

In our previous work [21], we studied classical magnetotransport and Shubnikov-de Haas (SdH) oscillations in this structure. It has been shown that the oscillations originate from topological electrons at the interface between HgTe and CdHgTe, as well as from 2D trivial electrons or holes and Volkov-Pankratov states, all confined within a gate-tunable accumulation layer [see Fig. 1(b)]. The low-mobility 3D electrons are located in the bulk and act as a separate classical conductivity channel. In contrast, here we focus on quantizing magnetic fields and demonstrate a distinct QHE characterized by several peculiar features, including the formation of a zero plateau in ρ_{xy}, quasiballistic edge channels on a macroscopic length scale, and anomalous scaling relative to the first electron plateau.

*Contact author: maksim.savchenko@silicon-austria.com

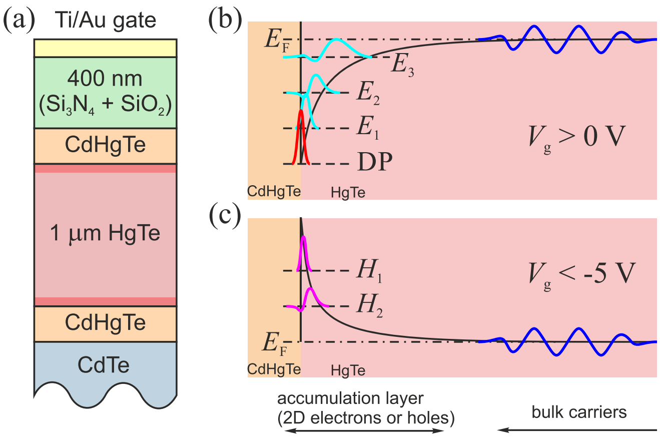

FIG. 1. (a) Schematic cross section of the structure under investigation. (b), (c) Proposed band diagram of the accumulation layer for positive and negative gate voltages, respectively. E_i and H_i denote the edges of the electron and hole subbands in the accumulation layer, DP is the Dirac point of the topological surface electrons, and E_F is the Fermi level.

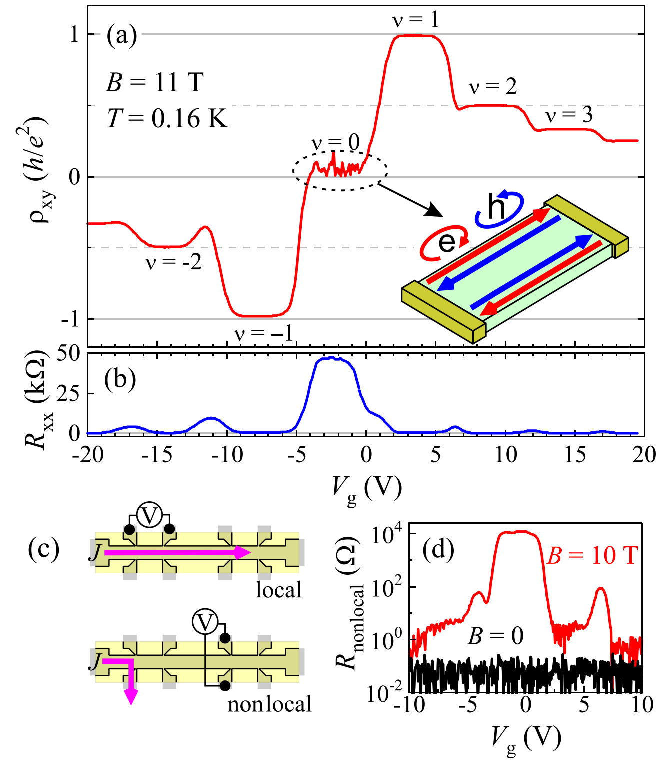

FIG. 2. (a) QHE plateaus in the Hall resistivity $\rho_{xy}(V_g)$ and (b) minima in the longitudinal resistance $R_{xx}(V_g)$ measured at $B = 11$ T and temperature $T = 0.16$ K. Note the formation of the zero plateau in ρ_{xy}. Inset: Schematic representation of counterpropagating chiral electron and hole edge channels. (c) Sketch of the macroscopic Hall bar with two measurement schemes: local (top, used for ρ_{xy} and R_{xx}) and nonlocal (bottom). The investigated Hall bars have a 50 μm wide current channel, with potential probes spaced 100 and 250 μm apart. (d) Nonlocal resistance vs gate voltage measured at $B = 0$ (black) and $B = 10$ T (red) at $T = 0.16$ K.

Figure 2(a) presents the main experimental result of our work: the Hall resistivity ρ_{xy} versus gate voltage V_g measured at $B = 11$ T shows clear plateaus on both the electron side (at positive V_g) and the hole side (at negative $V_g < -5$ V). The quantized values of ρ_{xy} correspond to h/e^2 and to its integer fractions. These plateaus in ρ_{xy} are accompanied by near-zero values of the diagonal resistance $R_{xx}(V_g)$, as shown in Fig. 2(b). Taken together, these observations provide compelling evidence for the emergence of a well-developed quantum Hall effect—an outcome that is particularly striking and unexpected in a three-dimensional system. All three devices studied exhibited consistent behavior. The centers of the plateaus are equally spaced in gate voltage, indicating that all two-dimensional carriers identified in Ref. [21] and shown in Figs. 1(b) and 1(c) contribute to the formation of the QHE and are hybridized by the strong magnetic field, a phenomenon previously observed in thinner HgTe films [7,19,22,23] and other systems [24]. Thus, the observed QHE is predominantly 2D in nature. Remarkably, however, the presence of a large number of bulk carriers does not appear to distort or suppress the formation of the QHE. We will revisit this point later.

At first glance, the behavior of R_{xx} and ρ_{xy} in Figs. 2(a) and 2(b) is similar to that observed in other electron-hole systems, such as graphene [2,9,25–27], or in closely related HgTe quantum wells [4,7,23,28–32]. In the quantum Hall regime, the centers of the ρ_{xy} plateaus generally align with minima in R_{xx} and σ_{xx}, as shown in Figs. 2(a) and 2(b) for $\nu \neq 0$. At the charge neutrality point (CNP), however, this correspondence breaks down: As the magnetic field increases and the temperature decreases, R_{xx} in most of the studied systems exhibits exponential growth and becomes significantly higher than h/e^2, while ρ_{xy} remains on the order of h/e^2 [2,4,9,25,29,33–40]. Consequently, $R_{xx} \gg \rho_{xy}$, causing both σ_{xx} and σ_{xy} to naturally approach zero as a result of inverting the resistivity tensor. In stark contrast, our system exhibits fundamentally different behavior: Near the CNP, we observe a zero plateau in the Hall resistivity ρ_{xy} accompanied by a maximum in $R_{xx} \lesssim 2h/e^2$. Although the zero σ_{xy} plateau is also observed in the system under investigation (see Fig. S3 of the Supplemental Material [41]), we emphasize the significance and uniqueness of the experimentally observing the zero plateau directly in the Hall resistivity ρ_{xy}. This behavior was consistently observed across all three investigated devices.

Unlike the plateaus at other filling factors, the zero Hall plateau in ρ_{xy} is not as precisely quantized. This is due to two main factors. First, extracting the plateau requires an antisymmetrization procedure to eliminate spurious contributions (see Fig. S5 of the Supplemental Material [41]). The need for antisymmetrization is expected, as the measured ρ_{xy} is invariably distorted by a component proportional to R_{xx}. Second, the zero plateau lacks precise quantization accuracy because the temperature is not identical at positive and negative B, which affects R_{xx} and, consequently, the obtained ρ_{xy} values. Together, these two effects lead to a shift and distortion of the plateau. Despite these variations, the exceptional nature of the zero plateau is evident, as its width and slope remain comparable with those of the other plateaus.

The unusual behavior of R_{xx} and ρ_{xy} near the CNP may be attributed to both bulk and edge conduction mechanisms. The absolute values of the diagonal resistance $R_{xx} \approx 2h/e^2$

at the CNP, along with its weak temperature dependence for $T < 0.2$ K (see Fig. S6 in the Supplemental Material [41]), suggest that the conduction mechanism originates from a disordered metal state, either in the bulk or at the edge. In the first scenario, the 2D conductivity is determined by the sum of partial contributions: electron and hole contributions are added for σ_{xx} but subtracted and cancel each other for σ_{xy} due to their opposite charges. In the second scenario, counterpropagating electron and hole channels form along the sample edges [4,8,9], resulting in a zero Hall resistivity. This is sketched in the inset of Fig. 2(a). Assuming the edge channels are dissipationless, the counterpropagating edge states result in a longitudinal resistance of $h/2e^2$ and a vanishing Hall resistance, as observed here—phenomenologically similar to the behavior of the quantum spin Hall effect (QSHE) [42]. The magnetic-field-induced QSHE state near the CNP was first predicted in Refs. [8,9,43] and later experimentally observed in graphene [44] as well as in HgTe quantum wells [4].

To determine which of these models best describes the system under study, we investigated the nonlocal transport properties of our sample. This method has been extensively used to demonstrate edge transport in both 2D TIs [45–52] and nontopological systems in the QHE regime [26,29,40,53–55]. For the nonlocal measurements, we separated the current and voltage pairs of the contacts by 350 μm, as shown in Fig. 2(c). The results of $R_{\text{nonlocal}}(V_g)$ measurements for magnetic fields of 0 and 10 T are shown in Fig. 2(d). The peak of the nonlocal resistance at the CNP at 10 T (red curve) provides clear evidence for the edge-based nature of the transport. The presence of even a small bulk conductivity (significantly smaller in magnitude than $1/R_{xx}$) will immediately lead to a reduction of the nonlocal resistance. This manifests itself, for example, in a steeper temperature dependence of the nonlocal resistance compared to the local one in the case of 2D TIs [49,50,52]. In the limiting case of dominant bulk conductivity, the theoretically expected value of the nonlocal resistance in the employed geometry should be exponentially small, on the order of $\rho_{xx}e^{-\pi L/W} \approx 10^{-10}\rho_{xx}$ (for more details, see Sec. S3 of the Supplemental Material [41]), with ρ_{xx} being the resistivity and $L/W = 7$ the geometrical length-to-width ratio of the corresponding section of the Hall bar. Such a situation is realized at $B = 0$, which results in a negligibly small measured signal [black curve in Fig. 2(d)]. This result clearly indicates that the zero-resistance plateau is formed by counterpropagating electron and hole channels, while the contribution of the bulk conductivity is negligible.

While edge transport is commonly observed in 2D electron-hole systems near the CNP and in the QHE regime [4,8,9,26,29,42,44], the observed low value of R_{xx} is unusual. In the above works, electron-hole edge channels in the QHE regime near CNP or in 2D TIs have no backscattering protection on scales larger than a few micrometers, leading to resistances much higher than h/e^2. In this context, the observed value of R_{xx} suggests that a quasiballistic transport regime is maintained over a scale of 100 μm, similar to the equilibration length of edge channels in the quantum Hall regime [56–58]. Quantitative estimates of the local and nonlocal resistance (see Sec. S3 of the Supplemental Material [41]) showed that the ballistic length of the edge states is at least 50 μm. The absence of a zero plateau in ρ_{xy} prior to antisymmetrization,

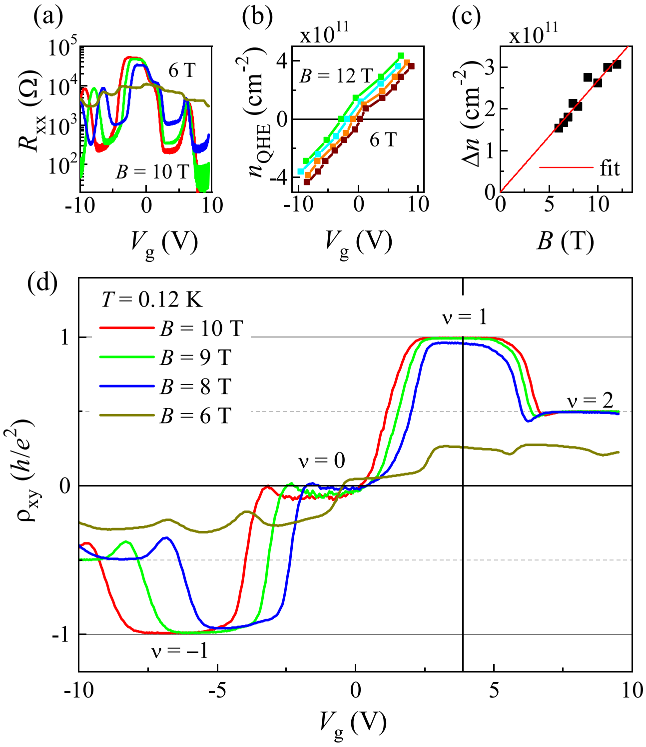

FIG. 3. Gate voltage dependences of (a) longitudinal and (d) Hall resistance in the QHE regime at magnetic fields of 6, 8, 9, and 10 T measured at $T = 0.12$ K. The gate voltage position of the first R_{xx} minimum and the corresponding ρ_{xy} plateau remains the same ($V_g =$ 4 V) regardless of the magnetic field, while all other minima and plateaus scale around $\nu = 1$ as the magnetic field changes. (b) Gate voltage dependence of the charge density n_{QHE} obtained from the positions of maxima and minima of R_{xx} for $B = 6$, 8, 10, and 12 T, respectively. Note the linear dependence of $n_{\text{QHE}}(V_g)$, as well as a linear shift between the curves in the magnetic field. (c) Gate-voltage-averaged charge-density shift $\Delta n(B) \equiv n_{\text{QHE}}(B) - n^{2D}_{\text{SdH}}$ taken from panel (b) and other QHE traces (not shown). Linear extrapolation to $B = 0$ gives $\Delta n = 0$, demonstrating the coincidence of n_{QHE} and n^{2D}_{SdH}.

combined with its strong temperature sensitivity, also indicated limited protection against backscattering. Further investigation is required to understand this issue in greater detail.

We now address the role of bulk 3D carriers by analyzing the evolution of the QHE in magnetic fields. Figures 3(a) and 3(d) show the magnetic field dependences of $R_{xx}(V_g)$ and $\rho_{xy}(V_g)$, respectively, in the range from 6 to 10 T. Starting at $B = 8$ T, well-defined plateaus in ρ_{xy} are visible and are accompanied by deep, flat minima in R_{xx}. For $\nu = 0$ near $V_g = 0$, R_{xx} exhibits a broad flat maximum with values between 30 and 50 kΩ. At lower magnetic fields, such as $B = 6$ T [brown trace in Fig. 3(d)], the QHE collapses abruptly. Instead of a gradual smearing of the plateaus, the values of $\rho_{xy}(V_g)$ deviate significantly from the quantized levels, and the overall shape of the traces loses resemblance to those observed at higher magnetic fields. Equally dramatic changes are observed in the gate voltage dependence of $R_{xx}(V_g)$ [Fig. 3(a)]: The clear oscillations vanish, giving way to a flatter profile with a much weaker dependence on gate voltage. The observed evolution of the QHE as a function of magnetic field is atypical, but can be well explained by the parallel conductivity of 3D carriers, which shunts the QHE state and distorts the observed traces. The density of the 3D carriers is expected to be independent of the gate voltage because of the screening, and therefore, the distortion is observed at all gate voltages. To be consistent with the observed evolution of the QHE traces, which show a qualitative change in the behavior as the magnetic field increases from 6 to 8 T, the conductivity of the 3D carriers has to decrease rapidly in a thresholdlike manner. A possible mechanism for this could be the localization of 3D carriers, either of the classical type, $\sigma_{xx} \propto 1/B^2$, or quantum localization, driven by disorder (when electrons are trapped in 3D puddles) and carrier interactions. At magnetic fields of 8 T and above, these carriers are expected to become almost fully localized, such that they no longer contribute significantly to the transport and thus cease to distort the R_{xx} and ρ_{xy} traces. Nevertheless, the influence of bulk carriers remains detectable at $B = 8$ T, as evidenced by the deviation of the ρ_{xy} plateau positions from $h/\nu e^2$, and the minima of R_{xx}, which saturate at a finite value instead of reaching zero. From the depth of these minima, and assuming the partial conductivity of the 2D carriers in the gap between Landau levels is negligible, we estimate that the bulk conductivity decreases from 10^{-6} to $10^{-7}\ \Omega^{-1}$ as the magnetic field increases from 8 to 10 T. More detailed insight into the localization of 3D carriers lies beyond the scope of the present work.

Localization of 3D carriers drives a transition from bulk to edge transport. Thus, the emergence of counterpropagating electron-hole edge channels and the zero Hall plateau cannot be strictly assigned to magnetic fields above 8 T. QHE traces at $B = 6$ T suggest that a QSHE-like state may already exist at lower fields, but its signatures are obscured by bulk conduction. This contrasts with graphene, where at the CNP strong magnetic fields induce a pseudospin ferromagnetic state [8,44,59], while bulk transport remains negligible and qualitative changes occur solely in edge channels. Fundamental differences between graphene and HgTe—including Zeeman energy scale, absence of valley degeneracy, carrier distribution along z, and dielectric screening—make a direct transfer of graphene-based symmetry-breaking mechanisms to HgTe unlikely.

The variation of the mobile carrier density with magnetic field is also reflected in the positions of the ρ_{xy} plateaus and the R_{xx} minima along the V_g axis. These positions correspond to integer-filled Landau levels, where the carrier density follows the standard quantum Hall relation $n_{\rm QHE} = \nu eB/h$. Due to the linear relationship between carrier density and gate voltage, the spacing ΔV_g between adjacent plateaus remains constant and is proportional to the magnetic field. Consequently, the ρ_{xy} and R_{xx} curves typically scale around the CNP [2,4,7,25,26,28,30]. However, the traces shown in Figs. 3(a) and 3(d) behave differently: As the magnetic field increases from 6 to 10 T, the position of the first electron plateau at $V_g =$ 4 V remains fixed, while the positions of the other plateaus (including the zeroth) scale linearly with the magnetic field relative to the first plateau. In other words, the first plateau serves as a reference point along the gate-voltage axis instead of the CNP. Since the electron density at the center of the first plateau is given by eB/h, this implies that the electron density at a fixed gate voltage varies with magnetic field. This behavior is verified throughout the full range of applied gate voltages. To illustrate this, Fig. 3(b) shows the dependence of $n_{\rm QHE}(V_g)$ extracted from the positions of the R_{xx} minima and maxima corresponding to integer and half-integer filling factors ν, for magnetic fields ranging from 6 to 12 T. All traces show linear dependencies with the identical slopes, but are offset relative to one another. The vertical separation between the curves represents the "excess" electron density, $\Delta n \equiv n_{\rm QHE} - n^{\rm 2D}_{\rm SdH}$, where $n^{\rm 2D}_{\rm SdH}$ is the 2D carrier density extracted from SdH oscillations (see Fig. S7 of the Supplemental Material [41]) in the limit of zero magnetic field. The resulting $\Delta n(B)$ follows a linear dependence starting from zero, as shown in Fig. 3(c), with a slope of $2.7 \times 10^{10}\ {\rm cm}^{-2}/{\rm T}$. The slope is close to e/h, which is precisely the value necessary to maintain the fixed gate voltage position of the first plateau and to scale the other plateaus relative to it. The excessive density only results from a redistribution of carriers from the 3D bulk to the 2D layer near the gate. Consequently, the reduction in bulk electron density enhances carrier localization in the bulk under a magnetic field and may even represent the dominant mechanism driving this localization for $B > 6$ T.

An exchange between quantized 2D carriers and a charge reservoir has previously been observed in HgTe quantum wells (QWs) [32,35,60] as well as in graphene [61], leading to anomalously extended Hall plateaus, a phenomenon known as the giant QHE. For such a transition to occur, the first electron LL must lie below the energy of the bulk electrons. This explanation is well founded, as the presence of a single LL with a negative slope, stemming from topological electrons, is a hallmark of HgTe QWs with an inverted energy spectrum [62,63]. To numerically support our explanation, we performed LL calculations using the eight-band $k \cdot p$ Hamiltonian [64]. The results reveal (see Sec. S1 of the Supplemental Material [41]) that the slope of the first electron LLs associated with the surface states is smaller than that of the bulk LLs. A more comprehensive theoretical model of the exchange processes remains to be developed.

The presented results raise several questions for future theoretical and experimental studies concerning the formation of the QHE and the potential to harness its unusually stable chiral edge states. The first issue is related to the role of bulk carriers. It would be particularly interesting to explore whether similar bulk electron localization occurs in other systems hosting both high-mobility and low-mobility carriers. Additionally, it remains unclear whether the observed linear e/h dependence of the excess density of 2D electrons on magnetic field persists in the strong field limit. Investigating the transport response of thicker HgTe films in quantizing magnetic fields may shed light on this problem. An intriguing possibility arising from such studies is the magnetically controlled separation of topological electrons located on opposite surfaces of the film. However, this hypothesis contrasts with experiments on thin strained HgTe films, where complete hybridization of electron states was observed in a strong magnetic field [23].

The second issue relates to the further investigation of the zero Hall resistance plateau. First, it is unclear whether the zero Hall resistance plateau can be observed in other systems. To address this issue, previously obtained experimental data should be re-examined. Second, we have found that the zero plateau is accompanied by the formation of electron-hole edge states. For reasons not yet understood, these states exhibit protection from backscattering over macroscopic distances, which is unusual in itself. It is logical to assume that protection from scattering is linked to the spatial separation of the electron and hole channels; however, it remains unclear whether this separation occurs along the z axis or within the plane of the sample, and to what extent bulk carriers play a role. Studying this problem may be of interest from the perspective of developing systems with a controlled degree of interaction between edge channels.

The financial support of this work by the Russian Science Foundation (Grant No. 23-72-30003), the European Research Council under the European Union's Horizon 2020 research and innovation program (Grant Agreement No. 787515, "ProMotion"), and Deutsche Forschungsgemeinschaft (DFG, German Research Foundation) via Project No. 521083032 (Ga501/19) is acknowledged.

Data availability. The data that support the findings of this Letter are not publicly available. The data are available from the authors upon reasonable request.

[1] K. v. Klitzing, G. Dorda, and M. Pepper, New method for high-accuracy determination of the fine-structure constant based on quantized Hall resistance, Phys. Rev. Lett. **45**, 494 (1980).

[2] J. G. Checkelsky, L. Li, and N. P. Ong, Zero-energy state in graphene in a high magnetic field, Phys. Rev. Lett. **100**, 206801 (2008).

[3] E. E. Mendez, L. Esaki, and L. L. Chang, Quantum Hall effect in a two-dimensional electron-hole gas, Phys. Rev. Lett. **55**, 2216 (1985).

[4] G. M. Gusev, E. B. Olshanetsky, Z. D. Kvon, N. N. Mikhailov, S. A. Dvoretsky, and J. C. Portal, Quantum Hall effect near the charge neutrality point in a two-dimensional electron-hole system, Phys. Rev. Lett. **104**, 166401 (2010).

[5] R. Yoshimi, A. Tsukazaki, Y. Kozuka, J. Falson, K. Takahashi, J. Checkelsky, N. Nagaosa, M. Kawasaki, and Y. Tokura, Quantum Hall effect on top and bottom surface states of topological insulator $(Bi_{1-x}Sb_x)_2Te_3$ films, Nat. Commun. **6**, 6627 (2015).

[6] Y. Xu, I. Miotkowski, C. Liu, J. Tian, H. Nam, N. Alidoust, J. Hu, C.-K. Shih, M. Z. Hasan, and Y. P. Chen, Observation of topological surface state quantum Hall effect in an intrinsic three-dimensional topological insulator, Nat. Phys. **10**, 956 (2014).

[7] J. Ziegler, D. A. Kozlov, N. N. Mikhailov, S. Dvoretsky, and D. Weiss, Quantum Hall effect and Landau levels in the three-dimensional topological insulator HgTe, Phys. Rev. Res. **2**, 033003 (2020).

[8] D. A. Abanin, P. A. Lee, and L. S. Levitov, Spin-filtered edge states and quantum Hall effect in graphene, Phys. Rev. Lett. **96**, 176803 (2006).

[9] D. A. Abanin, K. S. Novoselov, U. Zeitler, P. A. Lee, A. K. Geim, and L. S. Levitov, Dissipative quantum Hall effect in graphene near the Dirac point, Phys. Rev. Lett. **98**, 196806 (2007).

[10] S. Das Sarma and K. Yang, The enigma of the quantum Hall effect in graphene, Solid State Commun. **149**, 1502 (2009).

[11] D. V. Khveshchenko, Magnetic-field-induced insulating behavior in highly oriented pyrolitic graphite, Phys. Rev. Lett. **87**, 206401 (2001).

[12] Y. Ando, Topological insulator materials, J. Phys. Soc. Jpn. **82**, 102001 (2013).

[13] A. Bansil, H. Lin, and T. Das, *Colloquium:* Topological band theory, Rev. Mod. Phys. **88**, 021004 (2016).

[14] C. Brüne, C. X. Liu, E. G. Novik, E. M. Hankiewicz, H. Buhmann, Y. L. Chen, X. L. Qi, Z. X. Shen, S. C. Zhang, and L. W. Molenkamp, Quantum Hall effect from the topological surface states of strained bulk HgTe, Phys. Rev. Lett. **106**, 126803 (2011).

[15] E. J. König, P. M. Ostrovsky, I. V. Protopopov, I. V. Gornyi, I. S. Burmistrov, and A. D. Mirlin, Half-integer quantum Hall effect of disordered Dirac fermions at a topological insulator surface, Phys. Rev. B **90**, 165435 (2014).

[16] C. M. Wang, H.-P. Sun, H.-Z. Lu, and X. C. Xie, 3D quantum Hall effect of Fermi arcs in topological semimetals, Phys. Rev. Lett. **119**, 136806 (2017).

[17] F. Tang, Y. Ren, P. Wang, R. Zhong, J. Schneeloch, S. A. Yang, K. Yang, P. A. Lee, G. Gu, Z. Qiao, and L. Zhang, Three-dimensional quantum Hall effect and metal–insulator transition in $ZrTe_5$, Nature (London) **569**, 537 (2019).

[18] D. A. Kozlov, Z. D. Kvon, E. B. Olshanetsky, N. N. Mikhailov, S. A. Dvoretsky, and D. Weiss, Transport properties of a 3D topological insulator based on a strained high-mobility HgTe film, Phys. Rev. Lett. **112**, 196801 (2014).

[19] M. L. Savchenko, D. A. Kozlov, N. N. Vasilev, Z. D. Kvon, N. N. Mikhailov, S. A. Dvoretsky, and A. V. Kolesnikov, Topological surface states in thick partially relaxed HgTe films, Phys. Rev. B **99**, 195423 (2019).

[20] N. N. Berchenko and M. V. Pashkovskiĭ, Mercury telluride—A zero-gap semiconductor, Sov. Phys. Usp. **19**, 462 (1976).

[21] M. L. Savchenko, D. A. Kozlov, N. N. Vasilev, N. N. Mikhailov, S. A. Dvoretsky, and Z. D. Kvon, Transport properties of a 1000 nm HgTe film: The interplay of surface and bulk carriers, J. Phys.: Condens. Matter **35**, 345302 (2023).

[22] D. A. Kozlov, D. Bauer, J. Ziegler, R. Fischer, M. L. Savchenko, Z. D. Kvon, N. N. Mikhailov, S. A. Dvoretsky, and D. Weiss, Probing quantum capacitance in a 3D topological insulator, Phys. Rev. Lett. **116**, 166802 (2016).

[23] S. Hartl, L. Freund, M. Kühn, J. Ziegler, E. Richter, W. Himmler, J. Bärenfänger, D. A. Kozlov, N. N. Mikhailov, J. Weis, and D. Weiss, Quantum Hall effect and current distribution in the three-dimensional topological insulator HgTe, Phys. Rev. Res. **7**, 013273 (2025).

[24] M. Karalic, C. Mittag, S. Mueller, T. Tschirky, W. Wegscheider, K. Ensslin, T. Ihn, and L. Glazman, Phase slips and parity jumps in quantum oscillations of inverted InAs/GaSb quantum wells, Phys. Rev. B **99**, 201402 (2019).

[25] Y. Zhang, Z. Jiang, J. P. Small, M. S. Purewal, Y. W. Tan, M. Fazlollahi, J. D. Chudow, J. A. Jaszczak, H. L. Stormer, and P. Kim, Landau-level splitting in graphene in high magnetic fields, Phys. Rev. Lett. **96**, 136806 (2006).

[26] S. J. Hong, C. Belke, J. C. Rode, B. Brechtken, and R. J. Haug, Helical-edge transport near $\nu = 0$ of monolayer graphene, Curr. Appl. Phys. **27**, 25 (2021).

[27] J. Li, H. Fu, Z. Yin, K. Watanabe, T. Taniguchi, and J. Zhu, Metallic phase and temperature dependence of the $\nu = 0$ quantum Hall state in bilayer graphene, Phys. Rev. Lett. **122**, 097701 (2019).

[28] Z. D. Kvon, E. B. Olshanetsky, D. A. Kozlov, E. Novik, N. N. Mikhailov, and S. A. Dvoretsky, Two-dimensional semimetal in HgTe-based quantum wells, Low Temp. Phys. **37**, 202 (2011).

[29] G. M. Gusev, D. A. Kozlov, A. D. Levin, Z. D. Kvon, N. N. Mikhailov, and S. A. Dvoretsky, Robust helical edge transport at $\nu = 0$ quantum Hall state, Phys. Rev. B **96**, 045304 (2017).

[30] B. Büttner, C. X. Liu, G. Tkachov, E. G. Novik, C. Brune, H. Buhmann, E. M. Hankiewicz, P. Recher, B. Trauzettel, S. C. Zhang, and L. W. Molenkamp, Single valley Dirac fermions in zero-gap HgTe quantum wells, Nat. Phys. **7**, 418 (2011).

[31] A. Jost, M. Bendias, J. Böttcher, E. Hankiewicz, C. Brüne, H. Buhmann, L. W. Molenkamp, J. C. Maan, U. Zeitler, N. Hussey, and S. Wiedmann, Electron-hole asymmetry of the topological surface states in strained HgTe, Proc. Natl. Acad. Sci. USA **114**, 3381 (2017).

[32] D. A. Kozlov, J. Ziegler, N. N. Mikhailov, Z. D. Kvon, and D. Weiss, Spin splitting and disorder of Landau levels in HgTe-based Dirac fermions, Phys. Rev. B **108**, L241301 (2023).

[33] Z. Jiang, Y. Zhang, H. L. Stormer, and P. Kim, Quantum Hall states near the charge-neutral Dirac point in graphene, Phys. Rev. Lett. **99**, 106802 (2007).

[34] O. E. Raichev, G. M. Gusev, E. B. Olshanetsky, Z. D. Kvon, N. N. Mikhailov, S. A. Dvoretsky, and J. C. Portal, Unconventional Hall effect near charge neutrality point in a two-dimensional electron-hole system, Phys. Rev. B **86**, 155320 (2012).

[35] D. A. Kozlov, Z. D. Kvon, N. N. Mikhailov, and S. A. Dvoretsky, Quantum Hall effect in a system of gapless Dirac fermions in HgTe quantum wells, JETP Lett. **100**, 724 (2015).

[36] D. A. Kozlov, Z. D. Kvon, N. N. Mikhailov, S. A. Dvoretsky, S. Weishäupl, Y. Krupko, and J.-C. Portal, Quantum Hall effect in HgTe quantum wells at nitrogen temperatures, Appl. Phys. Lett. **105**, 132102 (2014).

[37] G. M. Gusev, E. B. Olshanetsky, Z. D. Kvon, A. D. Levin, N. N. Mikhailov, and S. A. Dvoretsky, Nonlocal transport near charge neutrality point in a two-dimensional electron-hole system, Phys. Rev. Lett. **108**, 226804 (2012).

[38] A. C. Lygo, B. Guo, A. Rashidi, V. Huang, P. Cuadros-Romero, and S. Stemmer, Two-dimensional topological insulator state in cadmium arsenide thin films, Phys. Rev. Lett. **130**, 046201 (2023).

[39] B. Guo, A. C. Lygo, X. Dai, and S. Stemmer, $\nu = 0$ quantum Hall state in a cadmium arsenide thin film, APL Mater. **10**, 091116 (2022).

[40] F. Nichele, A. N. Pal, P. Pietsch, T. Ihn, K. Ensslin, C. Charpentier, and W. Wegscheider, Insulating state and giant nonlocal response in an InAs/GaSb quantum well in the quantum Hall regime, Phys. Rev. Lett. **112**, 036802 (2014).

[41] See Supplemental Material at http://link.aps.org/supplemental/10.1103/fc7w-cq8f for Landau level calculations and additional data on local and nonlocal measurements in the quantum Hall regime.

[42] M. König, H. Buhmann, L. W. Molenkamp, T. Hughes, C.-X. Liu, X.-L. Qi, and S.-C. Zhang, The quantum spin Hall effect: Theory and experiment, J. Phys. Soc. Jpn. **77**, 031007 (2008).

[43] H. A. Fertig and L. Brey, Luttinger liquid at the edge of undoped graphene in a strong magnetic field, Phys. Rev. Lett. **97**, 116805 (2006).

[44] A. F. Young, J. D. Sanchez-Yamagishi, B. Hunt, S. H. Choi, K. Watanabe, T. Taniguchi, R. C. Ashoori, and P. Jarillo-Herrero, Tunable symmetry breaking and helical edge transport in a graphene quantum spin Hall state, Nature (London) **505**, 528 (2014).

[45] A. Roth, C. Brune, H. Buhmann, L. W. Molenkamp, J. Maciejko, X.-L. Qi, and S.-C. Zhang, Nonlocal transport in the quantum spin Hall state, Science **325**, 294 (2009).

[46] G. M. Gusev, Z. D. Kvon, O. A. Shegai, N. N. Mikhailov, S. A. Dvoretsky, and J. C. Portal, Transport in disordered two-dimensional topological insulators, Phys. Rev. B **84**, 121302(R) (2011).

[47] C. Brüne, A. Roth, H. Buhmann, E. M. Hankiewicz, L. W. Molenkamp, J. Maciejko, X.-L. Qi, and S.-C. Zhang, Spin polarization of the quantum spin Hall edge states, Nat. Phys. **8**, 485 (2012).

[48] G. M. Gusev, E. B. Olshanetsky, Z. D. Kvon, O. E. Raichev, N. N. Mikhailov, and S. A. Dvoretsky, Transition from insulating to metallic phase induced by in-plane magnetic field in HgTe quantum wells, Phys. Rev. B **88**, 195305 (2013).

[49] A. Rahim, A. D. Levin, G. M. Gusev, Z. D. Kvon, E. B. Olshanetsky, N. N. Mikhailov, and S. A. Dvoretsky, Scaling of local and nonlocal resistances in a 2D topological insulator based on HgTe quantum well, 2D Mater. **2**, 044015 (2015).

[50] E. B. Olshanetsky, Z. D. Kvon, G. M. Gusev, A. D. Levin, O. E. Raichev, N. N. Mikhailov, and S. A. Dvoretsky, Persistence of a two-dimensional topological insulator state in wide HgTe quantum wells, Phys. Rev. Lett. **114**, 126802 (2015).

[51] S. U. Piatrusha, E. S. Tikhonov, Z. D. Kvon, N. N. Mikhailov, S. A. Dvoretsky, and V. S. Khrapai, Topological protection brought to light by the time-reversal symmetry breaking, Phys. Rev. Lett. **123**, 056801 (2019).

[52] M. S. Ryzhkov, D. A. Khudaiberdiev, D. A. Kozlov, Z. D. Kvon, N. N. Mikhailov, and S. A. Dvoretsky, Edge and bulk transport in a two-dimensional topological insulator based on a CdHgTe quantum well, JETP Lett. **115**, 202 (2022).

[53] T. Morimoto, A. Furusaki, and N. Nagaosa, Charge and spin transport in edge channels of a $\nu = 0$ quantum Hall system on the surface of topological insulators, Phys. Rev. Lett. **114**, 146803 (2015).

[54] A. Nachawaty, M. Yang, S. Nanot, D. Kazazis, R. Yakimova, W. Escoffier, and B. Jouault, Large nonlocality in macroscopic Hall bars made of epitaxial graphene, Phys. Rev. B **98**, 045403 (2018).

[55] R. Brown, N. R. Walet, and F. Guinea, Edge modes and nonlocal conductance in graphene superlattices, Phys. Rev. Lett. **120**, 026802 (2018).

[56] B. W. Alphenaar, P. L. McEuen, R. G. Wheeler, and R. N. Sacks, Selective equilibration among the current-carrying states in the quantum Hall regime, Phys. Rev. Lett. **64**, 677 (1990).

[57] G. Müller, D. Weiss, A. V. Khaetskii, K. von Klitzing, S. Koch, H. Nickel, W. Schlapp, and R. Lösch, Equilibration length of electrons in spin-polarized edge channels, Phys. Rev. B **45**, 3932 (1992).

[58] G. Kirczenow and B. L. Johnson, Composite fermions, edge currents, and the fractional quantum Hall effect, Phys. Rev. B **51**, 17579 (1995).

[59] X. Liu, G. Farahi, C.-L. Chiu, Z. Papic, K. Watanabe, T. Taniguchi, M. P. Zaletel, and A. Yazdani, Visualizing broken symmetry and topological defects in a quantum Hall ferromagnet, Science **375**, 321 (2022).

[60] M. V. Yakunin, S. S. Krishtopenko, W. Desrat, S. M. Podgornykh, M. R. Popov, V. N. Neverov, S. A. Dvoretsky, N. N. Mikhailov, F. Teppe, and B. Jouault, Unconventional reentrant quantum Hall effect in a HgTe/CdHgTe double quantum well, Phys. Rev. B **102**, 165305 (2020).

[61] Z. R. Kudrynskyi, M. A. Bhuiyan, O. Makarovsky, J. D. G. Greener, E. E. Vdovin, Z. D. Kovalyuk, Y. Cao, A. Mishchenko, K. S. Novoselov, P. H. Beton, L. Eaves, and A. Patanè, Giant quantum Hall plateau in graphene coupled to an InSe van der Waals crystal, Phys. Rev. Lett. **119**, 157701 (2017).

[62] B. Scharf, A. Matos-Abiague, and J. Fabian, Magnetic properties of HgTe quantum wells, Phys. Rev. B **86**, 075418 (2012).

[63] O. E. Raichev, Effective Hamiltonian, energy spectrum, and phase transition induced by in-plane magnetic field in symmetric HgTe quantum wells, Phys. Rev. B **85**, 045310 (2012).

[64] S. S. Krishtopenko, I. Yahniuk, D. B. But, V. I. Gavrilenko, W. Knap, and F. Teppe, Pressure- and temperature-driven phase transitions in HgTe quantum wells, Phys. Rev. B **94**, 245402 (2016).